

Functionalisation of recombinant spider silk with conjugated polyelectrolytes

Christian Müller,^a Ronnie Jansson,^b Anders Elfving,^a Glareh Askarieh,^c Roger Karlsson,^d Mahiar Hamedi,^a Anna Rising,^b Jan Johansson,^b Olle Inganäs^a and My Hedhammar^b

Received 29th September 2010, Accepted 3rd December 2010

DOI: 10.1039/c0jm03270k

Conjugated polyelectrolytes are demonstrated to permit facile staining of recombinant spider silk fibres. We find that the polyelectrolyte concentration and pH of the staining solution as well as the incubation temperature strongly influence the efficiency of this self-assembly process, which appears to be principally mediated through favourable electrostatic interactions. Thus, depending on the choice of staining conditions as well as the polyelectrolyte, electrically conductive or photoluminescent recombinant silk fibres could be produced. In addition, staining of natural *Bombyx mori* silk is established, which emphasises the versatility of the here advanced approach to functionalise silk-based materials.

1. Introduction

Recombinant protein expression currently represents the most promising approach to realise biomaterials that mimic the attractive properties of natural spider silk,^{1–6} such as its outstanding mechanical properties^{7–10} and biocompatibility,^{11–13} as large-scale harvesting is complicated by the cannibalistic behaviour and low production levels of suitable spider species. Recently, considerable efforts have been devoted to further enhance the functionality of natural spider silk, as well as silk from silkworms, by *e.g.* surface-coating with inorganic nanoparticles,^{14–16} carbon nanotubes¹⁷ or *in situ* polymerisation of conjugated moieties,^{14,18} thereby inducing properties such as fluorescence,¹⁵ vapour sensing ability,¹⁶ magnetism¹⁴ or electrical conductivity.^{16–18} In a similar fashion, it may be desirable to equip the industrially more relevant recombinant silk fibres with additional qualities in order to facilitate advanced biomedical as well as bioelectronic applications. Thus, here we demonstrate that bulk-staining with conjugated polyelectrolytes readily renders this promising biomaterial electrically conducting, respectively, photoluminescent. Although these compounds are uniquely suited to functionalise polypeptide structures,^{19–22} so far, they have not been explored for their efficacy to decorate spider silk.

In particular, we elected to work with silk fibres prepared from the miniature recombinant spider silk protein 4RepCT

(Fig. 1a),^{5,23} which constitutes the C-terminal part of the dragline silk protein Major ampullate Spidroin 1 (MaSp1) of the African nursery web spider *Euprosthenops australis*. 4RepCT consists of four polyalanine and five glycine-rich segments followed by a non-repetitive C-terminal domain that was previously found to be crucial for *in vitro* fibre formation.^{23,24} Such recombinant silk fibres from 4RepCT currently constitute one of the most successful attempts to imitate their natural counterpart in terms of mechanical strength^{5,25} as well as biocompatibility.^{6,26,27}

These fibres we combine with the recently developed polyelectrolyte poly(4-(2,3-dihydrothieno[3,4-*b*]-[1,4]dioxin-2-yl-methoxy)-1-butananesulfonic acid) (PEDOT-S, Fig. 1b), which is water-soluble, self-doped, features a high electrical conductivity in the solid state²⁸ and readily binds to, *e.g.*, β -sheet rich amyloid fibrils.²² In addition, the related conjugated polymer poly(3,4-ethylenedioxythiophene) (PEDOT) has been reported to be biologically benign^{29,30} and thus PEDOT-S is likely to display a similar level of biocompatibility.

In particular we find that under appropriate conditions, PEDOT-S readily self-assembles onto 4RepCT fibres, which as a result display an appreciable level of electrical conductivity. Furthermore, in order to demonstrate the general applicability of the here introduced method to functionalise silk-based materials, we explore the self-assembly process of the photoluminescent polyelectrolyte poly(thiophene acetic acid) (PTAA) onto 4RepCT fibres. Using the same protocols, we could also successfully stain natural silk fibres from the silkworm *Bombyx mori*.

2. Results and discussion

Self-assembly of PEDOT-S onto 4RepCT fibres

In order to establish the affinity of the polyelectrolyte to bind to 4RepCT recombinant silk, in a first set of experiments we

^aBiomolecular and Organic Electronics, Department of Physics, Chemistry & Biology, Linköping University, 58183 Linköping, Sweden. E-mail: christian.muller@ifm.liu.se

^bDepartment of Anatomy, Physiology and Biochemistry, SLU, Biomedical Centre, 751 23 Uppsala, Sweden. E-mail: my.hedhammar@afb.slu.se

^cDepartment of Molecular Biology, Uppsala BioCenter, SLU, Biomedical Centre, 751 24 Uppsala, Sweden

^dDepartment of Physics, Chemistry & Biology, Linköping University, 58183 Linköping, Sweden

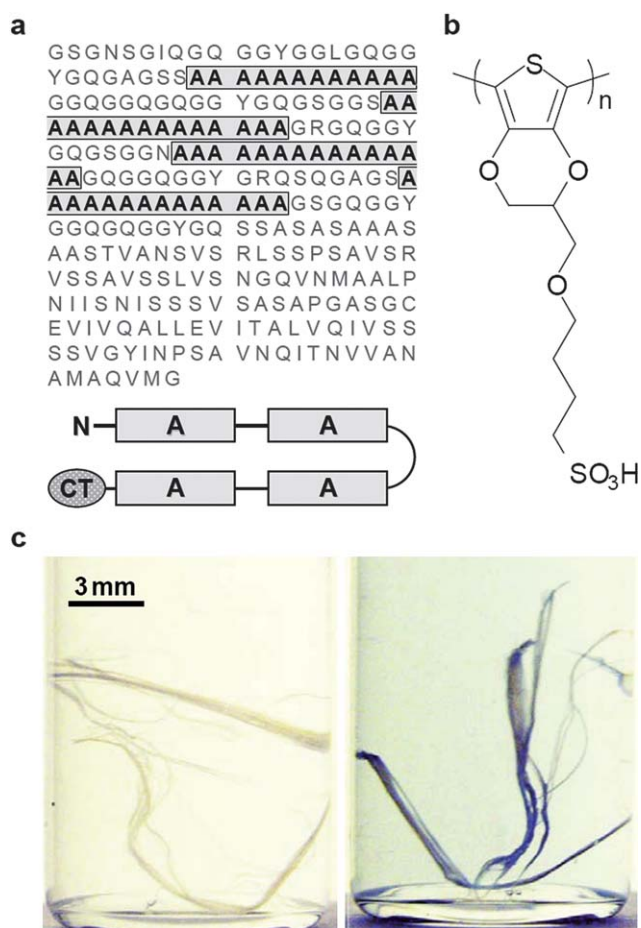


Fig. 1 (a) Primary sequence as well as a schematic representation of the recombinant spider silk protein 4RepCT comprising four repetitive polyalanine stretches (A), five glycine-rich segments (thin lines) and the C-terminal domain (CT) (*cf.* ref. 5 and 23). (b) Chemical structure of PEDOT-S. (c) Optical micrographs of recombinant spider silk fibres that have been immersed for two weeks at ambient temperature in water (left) or dilute (0.1 g L^{-1}) aqueous PEDOT-S solution (right).

submersed these fibres in water that contained various concentrations of PEDOT-S. Indeed, we found that given sufficient time, initially white fibres adopted a deep blue colour, indicative of efficient interaction of the two materials (Fig. 1c), which appeared favourable even if the fibres were subsequently rinsed with or incubated in distilled water. The rate of this self-assembly process could be significantly enhanced by both an increase in PEDOT-S concentration as well as elevated incubation temperature. Thus, efficient staining was accomplished after only one hour at 90°C in more concentrated solutions (10 g L^{-1} PEDOT-S in water). It is important to note that due to the acidic nature of the polyelectrolyte these solutions displayed a pH of down to 2.

With the aim to further elucidate the nature of the PEDOT-S/4RepCT interaction, we varied the pH of the staining solution between pH 2 and 13 using a Britton–Robinson buffer system (*cf.* Experimental). The theoretical isoelectric point (pI) of the soluble 4RepCT is situated around 8.9.²³ Thus, at very basic conditions, *i.e.* pH > 8.9, 4RepCT fibres can be expected to be negatively charged. At the same basic conditions, the butanesulfonate side chains of PEDOT-S are strongly dissociated and thus carry a negative charge, whereas the polymer backbone is

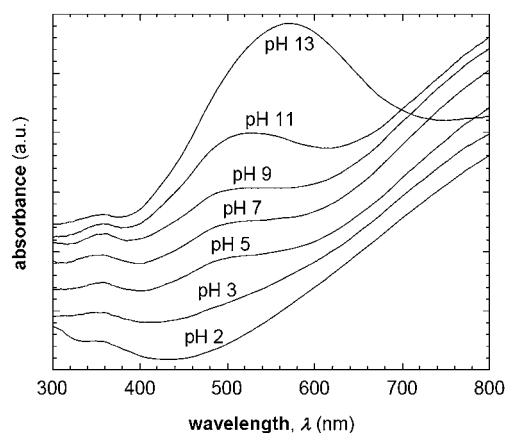


Fig. 2 UV-vis absorbance spectra of dilute (0.2 g L^{-1}) PEDOT-S solutions; the pH was adjusted between 13 and 2 as indicated. Note that for pH < 3, the polymer is completely oxidised as evidenced by the absence of the π - π^* absorption at 500–600 nm (*cf.* ref. 28).

present in its neutral form, as evidenced by the dark purple colour of PEDOT-S solutions, which results from absorption by the π - π^* transition at 500–600 nm (Fig. 2).²⁸ As a consequence, blue fibres that were previously stained with PEDOT-S at pH 2 gradually lose their colour when incubated in a buffer at pH 13, suggesting that under these conditions interaction of 4RepCT with the polyelectrolyte is, in fact, highly unfavourable and reversible, likely due to strong electrostatic repulsion. However, recombinant silk fibres could be marginally stained at pH 11 even though both 4RepCT and PEDOT-S are expected to be negatively charged under these conditions, suggesting that other, non-electrostatic interactions become more noticeable. Hydrogen-bonding, aromatic π -stacking, as well as hydrophobic and quasi-epitaxial interactions have been suggested to contribute to the binding of conjugated electrolytes to various polypeptide-based structures,^{31,32} which may also play a role for the system at hand. The relevance of such modes of interaction is given weight by reports demonstrating that besides ionic interactions especially the degree of conjugation of various organic dyes influences their propensity to colour natural silk fibres.^{33,34}

When lowering the pH, the butanesulfonate side chains of PEDOT-S, which remain negatively charged, start to act as counterions for the increasingly oxidised and thus positively charged polymer backbone.³⁵ [Note that due to the very low $\text{pK}_a < 0$ of sulfonic acid derivatives, these side chains display a pH-independent electrochemistry for the here investigated pH range (*cf.* ref. 35).] It is this self-doping process that renders the polyelectrolyte electrically conductive. The increasing oxidation of the backbone is consistent with the gradual loss of π - π^* absorption and the resulting colour shift of PEDOT-S solutions from dark purple to deep blue when decreasing the pH from 13 to 2, resulting in a completely oxidised backbone for pH < 3 (*cf.* Fig. 2). Thus, with decreasing pH, PEDOT-S can be expected to remain negatively charged but approach charge neutrality, whereas 4RepCT will carry an increasingly positive charge for pH < pI. Therefore, we studied dyeing over a wide pH range (*i.e.* pH 11 to 2) and observed that the propensity of PEDOT-S to stain 4RepCT fibres gradually increased when lowering the pH, as judged subjectively by the resulting depth of colour. At a very low pH (~ 2) most efficient staining with PEDOT-S was achieved,

Table 1 Mechanical properties and electrical conductivity of 4RepCT/PEDOT-S fibres and for comparison pristine 4RepCT fibres as well as spin-coated PEDOT-S thin films: Young's modulus E , fractures stress σ_{fracture} and electrical conductivity c (errors were estimated through comparison of n similar samples). [Note that the here reported fracture stress probably does not correspond to the material's ultimate tensile strength as fibres often failed at the grip point; the fragility of fibres complicated handling and is likely to have weakened samples prior to mechanical testing, e.g. during fixation.] Samples were prepared at the indicated pH, temperature T (a.t. = ambient temperature) and staining time t ; '—' denotes not measured

Sample	Preparation			Tensile testing			Conductivity	
	pH	$T/^\circ\text{C}$	t	n	E/GPa	$\sigma_{\text{fracture}}/\text{MPa}$	n	$c^a/\text{S cm}^{-1}$
4RepCT	7	a.t.	—	5	6.5 ± 1.4	89 ± 9	2	$<10^{-7}$
4RepCT/PEDOT-S	2	a.t.	10–14 d	6	5.6 ± 2.1	61 ± 29	3	$(7 \pm 2) \times 10^{-5}$
4RepCT/PEDOT-S	2	90	1–2 h	2 ^b	5.9, 6.9	61, 85	6	$(8 \pm 2) \times 10^{-4}$
4RepCT/PEDOT-S	3–11	a.t.	14 d	—	—	—	1 ^c	$<10^{-7}$
PEDOT-S	2	a.t.	—	—	—	—	4	18 ± 4

^a $c < 10^{-7} \text{ S cm}^{-1}$ was not accessible because of experimental limitations. ^b The majority of fibres fractured prematurely during handling. ^c One sample each for pH 3, 5, 7, 9, and 11.

aided by now favourable electrostatic interactions (*cf.* Table 1). [Note that quantitative means such as UV-vis or fluorescence spectroscopy were not practical for this set of samples because of the poor optical response of the doped PEDOT-S.]

Microstructure and mechanical properties of PEDOT-S stained 4RepCT fibres

The dried 4RepCT fibres are composed of a multitude of tightly packed filaments with a diameter of approximately 30–200 nm.^{5,36} Similar to other silk structures, on a molecular level they consist of β -sheet crystallites that are embedded in a more disordered, *i.e.* amorphous matrix.^{1,7–9} Necessary structural cross-links are provided by such β -sheet crystallites as well as hydrogen-bonding in amorphous domains. This is in agreement with our observation that 4RepCT fibres have to be dried under tension in order to maximise their mechanical strength, a procedure which is known to promote formation of hydrogen-bonds between partially aligned amorphous peptide sections (*cf.* ref. 8).

The structure and distribution of hydrophobic β -sheet crystallites was found to be little affected by the staining process, as evidenced by X-ray diffractograms of pristine as well as PEDOT-S stained 4RepCT fibres displayed in Fig. 3a. This is in agreement with our recent observation that the microstructure of pristine fibres is not affected by autoclaving at 121 °C (*cf.* ref. 27). Diffractions are present as full circles, indicating that crystalline domains are mostly unoriented within monofilaments. Furthermore, various diffractions are consistent with the β -poly(L-alanine) but also poly(L-alanyl-glycine) structure,³⁷ suggesting that it is in particular the polyalanine segments of 4RepCT that form β -sheet crystallites (Fig. 3b).

Most significantly, we found that our 4RepCT fibres were stained with PEDOT-S throughout the bulk as evidenced by optical microscopy on fibre cross-sections (Fig. 3c). Certainly, the polyelectrolyte can efficiently enter the free volume between filaments but, in addition, may also penetrate water-soaked amorphous regions. Water uptake by amorphous regions is corroborated by the swelling of fibres when soaked in water, which resulted in a reversible extension of the fibre length (Fig. 3d; also *cf.* ref. 9). Wet fibres were found to be reasonably flexible whereas dried fibres appeared to be more stiff and fragile (*cf.* ref. 5). The stiffness and brittleness of dried fibres is also reflected by the high Young's modulus E and linear

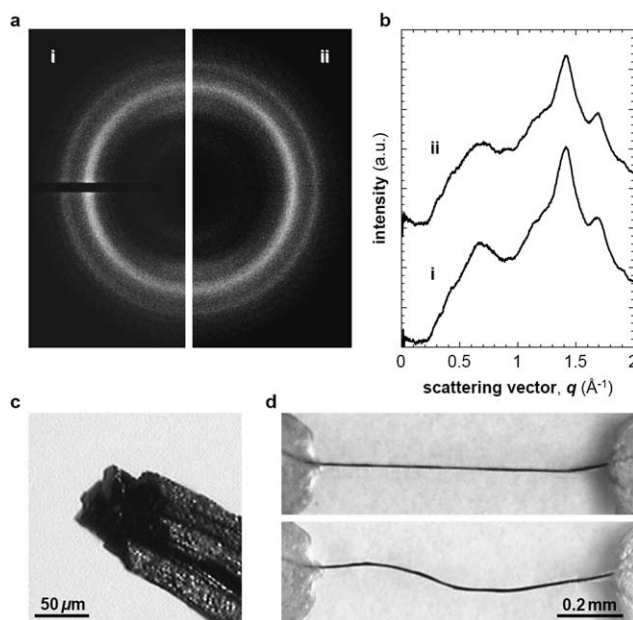


Fig. 3 (a) Transmission wide-angle X-ray diffraction patterns of a pristine 4RepCT fibre (i) and a fibre stained with PEDOT-S for two hours at $\text{pH} \approx 2$ and 90°C (ii). (b) Corresponding radially integrated X-ray diffractograms. (c) Optical micrograph of a cross-section of a cut PEDOT-S stained fibre. (d) A dry PEDOT-S stained fibre fixed with silver paste (top) elongates and curls upon wetting (bottom).

stress–elongation relationship with no obvious yielding point as revealed by tensile deformation experiments (Fig. 4). Unfortunately, we found that dried PEDOT-S stained fibres were even more fragile than pristine fibres during handling. This observation is in agreement with the apparent decrease in fracture stress σ_{fracture} upon staining with PEDOT-S: pristine 4RepCT fibres fractured at $\sigma_{\text{fracture}} \approx 89 \pm 9 \text{ MPa}$, whereas for instance fibres stained with PEDOT-S at $\text{pH} 2$ and ambient temperature failed at $\sigma_{\text{fracture}} \approx 61 \pm 29 \text{ MPa}$ (Fig. 4 and Table 1). [Note that a Student's t -test between these two values yielded a probability value $p = 0.063$, indicating a limited statistical relevance.] This increase in brittleness of the dried PEDOT-S stained fibres is consistent with the picture that the polyelectrolyte had in part intercalated between amorphous 4RepCT segments and thus partially inhibited hydrogen bond formation. Moreover, it

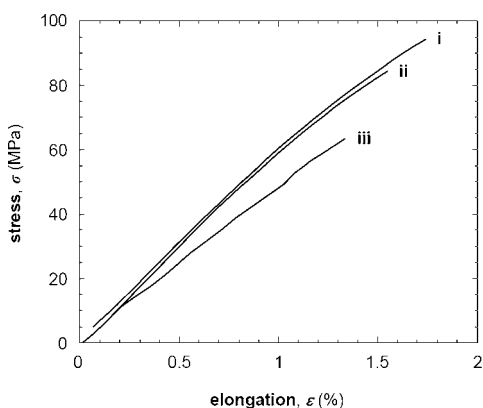


Fig. 4 Stress–elongation curves of a representative pristine 4RepCT fibre (i), a fibre stained with PEDOT-S for two hours at pH 2 and 90 °C (ii) or for 14 days at pH 2 and ambient temperature (iii).

should be noted that the dried stained fibres regained their flexibility if wetted again, comparable to the behaviour of pristine fibres. We rule out that the used staining conditions affect the mechanical properties of 4RepCT fibres because of their remarkable stability during autoclaving at 121 °C as discussed above.²⁷ Here, it is interesting to note that dyeing of natural silk fibres is often found to result in a slight deterioration of their mechanical properties,^{38,39} especially if reactive dyes are employed.⁴⁰ Although the hydrodynamic radius of PEDOT-S particles in water is at the order of at least 2 nm,²⁸ we suggest that PEDOT-S can to some extent diffuse into amorphous regions of 4RepCT if given enough time, which will gradually provide access to the charged surfaces of the protein. In fact, the long time required to achieve good staining of 4RepCT fibres is consistent with this picture. As a result, besides coating the surface of filaments, PEDOT-S may be found within positively charged amorphous regions or adhere to the surface of electrically neutral and hydrophobic polyalanine β -sheet crystallites, as has been suggested for PEDOT-S/amyloid fibril complexes from insulin.²²

Electrical conductivity of PEDOT-S stained 4RepCT fibres

As we set out to produce electrically conducting recombinant silk, in a further set of experiments we examined PEDOT-S stained 4RepCT fibres for their electrical properties. Gratifyingly, we found that fibres stained at a sufficiently low pH, *i.e.* pH 2, displayed an electrical conductivity $c \approx (7 \pm 2) \times 10^{-5} \text{ S cm}^{-1}$ if treated at ambient temperature, whereas staining at 90 °C resulted in $\sigma \approx (8 \pm 2) \times 10^{-4} \text{ S cm}^{-1}$ (Fig. 5 and Table 1). This unfavourably compares with the conductivity of PEDOT-S thin films, which we measured to be $18 \pm 4 \text{ S cm}^{-1}$. However, some of this discrepancy can be accounted for by considering that the conductivity of fibres was estimated with respect to their cross-sectional area and thus disregards the presence of a majority fraction of the insulating 4RepCT material (*cf.* Experimental). In addition, it is important to note that the polyelectrolyte used in this study was of rather low molecular weight,²⁸ the increase of which can be expected to strongly enhance percolation of charge-transport pathways along the fibre and thus electrical conductivity, especially if only a small amount of the conjugated

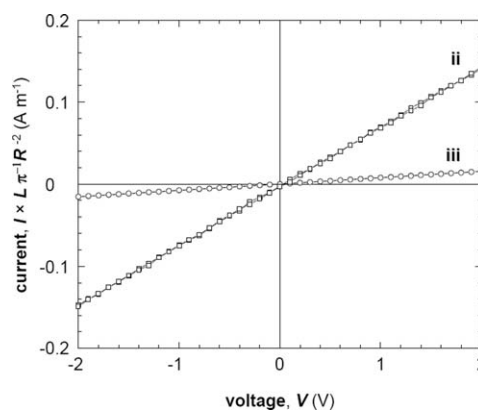


Fig. 5 Representative ohmic current–voltage, I – V , characteristics of recombinant spider silk fibres stained with PEDOT-S for one hour at pH 2 and 90 °C (ii) or for 10 days at pH 2 and ambient temperature (iii). The current was normalised with respect to the length, L , of the conducting fibre segment as well as the approximate cross-sectional area, πR^2 , where R is the mean radius. Note that pristine 4RepCT fibres (i) displayed no measurable conductivity.

material is bound. In stark contrast, staining at pH > 2 and ambient temperature appeared to result in incorporation of a significantly lower amount of PEDOT-S, even when extending the staining process to several weeks, as suggested by the absence of measurable electrical conductivity (Table 1). Acidic post-treatment of fibres that had been stained at pH > 2 did not result in more conductive fibres, confirming that the lack of sufficient PEDOT-S incorporation and not inadequate doping of the polymer likely is the explanation for this observation (*cf.* Fig. 2).

Use of other polyelectrolytes/silk structures

In order to demonstrate the general applicability of the here discussed approach to functionalise recombinant spider silk, we also stained fibres with poly(thiophene acetic acid) (PTAA).^{21,31} In this way photoluminescent fibres could readily be produced as illustrated by the fluorescence micrograph and spectra presented in Fig. 6. Similar to staining with PEDOT-S discussed above, most efficient decoration of 4RepCT fibres with PTAA was achieved after staining for two hours at 90 °C. Conversely, at ambient temperature this process required considerably more time; for instance one week at pH 7 was needed to reach a similar level of fluorescence. Again, the pH of staining solutions was found to be crucial. PTAA only dissolved in appreciable quantities at pH ≥ 6 , which can be rationalised with the $pK_a \approx 4.8$ of acetic acid. Thus, we performed staining experiments in the range of pH 7–11. As evidenced by the fluorescence spectra of PTAA stained 4RepCT fibres in Fig. 6b, at pH 7–9 PTAA displayed a strong affinity for 4RepCT. In most significant contrast, attempts to decorate fibres with PTAA at pH 10 resulted in a ~ 30 times lower fluorescence as compared to fibres stained at pH 7. Ultimately, at pH 11 fluorescence from PTAA was found to be virtually absent. Evidently, the $pI \approx 8.9$ of 4RepCT strongly influenced binding of PTAA. For pH < 8.9, a strong attraction between 4RepCT, which carries a net positive charge, and the negatively charged side chains of PTAA can be expected, highlighting the dominance of electrostatic interactions between the conjugated polyelectrolyte and protein. However, a weak

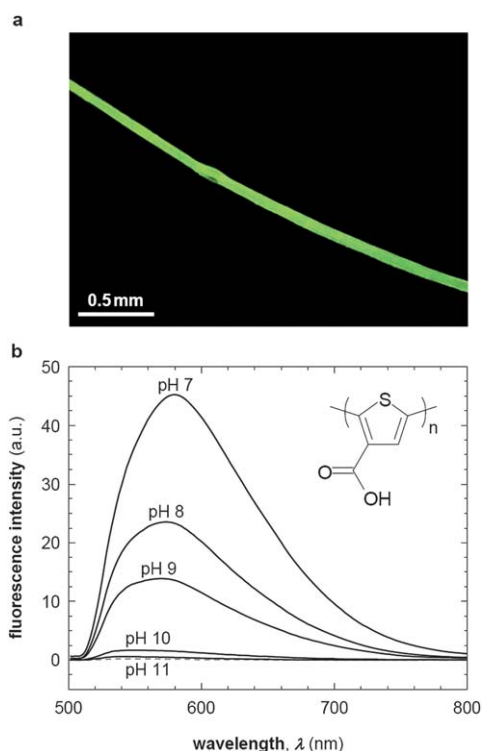


Fig. 6 (a) Fluorescence micrograph of a recombinant silk fibre stained with PTAA for two hours at 90 °C and pH 9. (b) Fluorescence spectra of fibres stained for two hours at 90 °C and the indicated pH (solid lines) as well as of a pristine 4RepCT fibre (dashed line). The inset shows the chemical structure of PTAA.

interaction still appeared to be present in more alkaline solutions, *i.e.* at pH 10, suggesting that other modes of binding may also contribute to the attachment of PTAA to 4RepCT fibres, which can to some extent overcome the electrostatic repulsion between the two now negatively charged species.

The here proposed method to functionalise 4RepCT fibres could also be extended to other silk structures, such as solution-cast 4RepCT thin films as well as natural silk fibres from the silkworm *B. mori*. Gratifyingly, we found that also PEDOT-S stained *B. mori* fibres displayed an electrical conductivity of at least 10^{-3} S cm^{-1} when stained at elevated temperature and low pH (90 °C and pH 2).

3. Conclusions

The combination of recombinant spider silk and conjugated polyelectrolytes such as PEDOT-S and PTAA permitted us to equip this highly versatile biomaterial with novel bulk-electrical and optical properties. The generality of this approach was illustrated by demonstrating its applicability also to natural silk fibres from the silkworm *B. mori*. Clearly, the here proposed method based on a self-assembly process may prove highly useful in future biomedical and bioelectronic applications, such as the growth of stem or nerve cells on three-dimensional conducting templates,^{41–44} as well as the realisation of biocompatible actuators,⁴⁵ electronic sensors and textile-based electrodes.⁴⁶

4. Experimental

Materials

Poly(4-(2,3-dihydrothieno[3,4-*b*]-[1,4]dioxin-2-yl-methoxy)-1-butananesulfonic acid, sodium salt) (PEDOT-S) and poly-(thiophene acetic acid) (PTAA) were synthesised according to the previously reported procedures.^{28,47} Aqueous solution of the sodium salt PEDOT-S polymer was stirred with Dowex Marathon C cation exchange resin to obtain the sulfonic acid form. Then, PEDOT-S was loaded on a PD-10 size exclusion column (Sephadex™ G-25 M) in 3 mL batches and eluted with 3 mL of water. Finally, PEDOT-S was dialysed against de-ionized water for two days using a 3500 g mol^{-1} cut-off membrane (Spectra/Por) and freeze-dried prior to use. The yield was ~45% with respect to the monomer unit.

Preparation of the recombinant miniature spider silk protein 4RepCT (23.4 kDa) as well as fabrication of fibres therewith have been reported elsewhere.^{5,23} Degummed silk fibres from the silkworm *B. mori* were used as received.

Sample preparation

For photographs of fibres, structures were stained with PEDOT-S by suspension in water (0.1 g L^{-1} PEDOT-S) for two weeks at ambient temperature.

For electrical conductivity and tensile deformation measurements on solid fibres, structures were first dried under tension at ambient temperature. Staining with PEDOT-S was achieved by submerging these fibres in water (10 g L^{-1} PEDOT-S) for up to 15 days at ambient temperature or 1–2 hours at 90 °C, subsequent to which the fibres were washed with distilled water and again dried under tension. The pH of PEDOT-S and PTAA solutions was adjusted using a Britton–Robinson buffer system (0.04 M H_3BO_3 , 0.04 M H_3PO_4 and 0.04 M CH_3COOH titrated with 0.2 M NaOH), which permitted buffering in the range of pH 2 to 12. pH 13 was reached with 0.2 M NaOH.

Staining with PTAA was achieved by submersion of fibres in water (0.1 g L^{-1} PTAA) for one week at ambient temperature or 90 °C for two hours, subsequent to which the fibres were washed with distilled water.

pH determination

The pH of PEDOT-S and PTAA solutions was determined with a Biotrode pH-meter (Mettler Toledo). The theoretical net charge of soluble 4RepCT was calculated using www.expasy.ch/tools, yielding an isoelectric point $\text{pI} \approx 8.9$ (*cf.* ref. 23; 4RepCT carries a net positive charge for $\text{pH} < \text{pI}$ and a net negative charge for $\text{pH} > \text{pI}$).

Optical microscopy

Optical microscopy was carried out with a Nikon SMZ 1000 stereomicroscope equipped with a Sony Exwave HAD camera.

Ultraviolet-visible light (UV-vis) absorbance spectroscopy

UV-vis absorbance spectra of PEDOT-S solutions (0.2 g L^{-1} ; quartz cuvette with 1 mm path length) were recorded using a Perkin Elmer Lambda 950 UV-vis spectrophotometer.

X-Ray diffraction

Transmission wide-angle X-ray diffraction was carried out with an in-house rotating anode instrument using CuK α -radiation ($\lambda = 1.5418 \text{ \AA}$).

Differential Mechanical Analysis (DMA)

Mechanical testing of fibers with a radius $R \approx 20\text{--}50 \text{ }\mu\text{m}$ was performed at ambient temperature with a TA Instruments DMA Q800 V7.4 analyser using a ramp force of 0.2 N min^{-1} . The gauge length of 0.8 cm was ensured by gluing fibres with cyanoacrylate (LoctiteVR Super AttakVR) to a double paper frame that was subsequently mounted in the tensile cell and released before measurements. Fibres that displayed macroscopic defects or appeared to suffer during mounting were excluded. A circular cross-section was assumed to calculate the stress.

Electrical conductivity measurements

PEDOT-S stained fibres were contacted with silver paste (Agar Scientific) and two-point electrical conductivity measurements were performed with a Keithley 4200 parameter analyser on fibre segments with a typical length $L \approx 0.5\text{--}1 \text{ cm}$ and radius $R \approx 20\text{--}70 \text{ }\mu\text{m}$. 4-Point probe measurements (1 mm probe spacing) on particularly thick fibres were used to confirm the electrical conductivities estimated from two-point measurements as well as to determine the conductivity of $60\text{--}80 \text{ nm}$ thick spin-coated PEDOT-S thin films.

The electrical conductivity c was estimated as

$$c = \frac{I}{V} \times \frac{L}{\pi R^2}$$

where I is the measured current and V the applied voltage; L and R are the individual dimensions of fibres.

Fluorescence microscopy

Fluorescence microscopy was carried out with an A200 Zeiss Axiovert inverted epifluorescence microscope equipped with a CCD camera (AxioCam HRC 3-chip), using a $470/40 \text{ nm}$ filter (LP1515). Fluorescence spectra were recorded with a SpectraCube SD-300 VDS system. The fluorescence spectra of PTAA stained 4RepCT fibres were corrected for the fibre diameter.

Acknowledgements

We would like to acknowledge funding from the Swedish Foundation for Strategic Research (SSF) through the programme Organic hybrid Printed Electronics and Nanoelectronics (OPEN), Vinnova, Formas and The Swedish Research Council.

References

- 1 J. O. O'Brien, S. R. Fahnestock, Y. Termonia and K. C. H. Gardner, *Adv. Mater.*, 1998, **10**, 1185–1195.
- 2 A. Lazaris, S. Arcidiacono, Y. Huang, J.-F. Zhou, F. Duguay, N. Chretien, E. A. Welsh, J. W. Soares and C. N. Karatzas, *Science*, 2002, **295**, 472–476.
- 3 S. Arcidiacono, C. M. Mello, M. Butler, E. Welsh, J. W. Soares, A. Allen, D. Ziegler, T. Laue and S. Chase, *Macromolecules*, 2002, **35**, 1262–1266.
- 4 J. H. Exler, D. Hümmerich and T. Scheibel, *Angew. Chem., Int. Ed.*, 2007, **46**, 3559–3562.
- 5 M. Stark, S. Grip, A. Rising, M. Hedhammar, W. Engström, G. Hjälml and J. Johansson, *Biomacromolecules*, 2007, **8**, 1695–1701.
- 6 A. Rising, M. Widhe, J. Johansson and M. Hedhammar, *Cell. Mol. Life Sci.*, 2010, DOI: 10.1007/s00018-010-0462-z.
- 7 M. Denny, *J. Exp. Biol.*, 1976, **65**, 483–506.
- 8 Y. Termonia, *Macromolecules*, 1994, **27**, 7378–7381.
- 9 J. M. Gosline, P. A. Guerette, C. S. Ortlepp and K. N. Savage, *J. Exp. Biol.*, 1999, **202**, 3295–3303.
- 10 C. Riekel, B. Madsen, D. Knight and F. Vollrath, *Biomacromolecules*, 2000, **1**, 622–626.
- 11 F. Vollrath, P. Barth, A. Basedow, W. Engström and H. List, *In Vivo*, 2002, **16**, 229–234.
- 12 C. Allmeling, A. Jokuszies, K. Reimers, S. Kall, C. Y. Choi, G. Brandes, C. Kaspar, T. Scheper, M. Guggenheim and P. M. Vogt, *Cell Proliferation*, 2008, **41**, 408–420.
- 13 Y. Yang, X. Chen, F. Ding, P. Zhang, J. Liu and X. Gu, *Biomaterials*, 2007, **28**, 1643–1652.
- 14 E. L. Mayes, F. Vollrath and S. Mann, *Adv. Mater.*, 1998, **10**, 801–805.
- 15 M. Chu and Y. Sun, *Smart Mater. Struct.*, 2007, **16**, 2453–2456.
- 16 A. Singh, S. Hede and M. Sastry, *Small*, 2007, **3**, 466–473.
- 17 H. S. Kim, M. Kang, H.-J. Jin, I.-J. Chin, H. J. Choi and J. Joo, *Mol. Cryst. Liq. Cryst.*, 2007, **464**, 15–21.
- 18 Y. Xia and Y. Lu, *Compos. Sci. Technol.*, 2008, **68**, 1471–1479.
- 19 K. P. R. Nilsson, J. Rydberg, L. Baltzer and O. Inganäs, *Proc. Natl. Acad. Sci. U. S. A.*, 2004, **101**, 11197–11202.
- 20 A. Herland, P. Björk, K. P. R. Nilsson, J. D. M. Olsson, P. Åsberg, P. Konradsson, P. Hammarström and O. Inganäs, *Adv. Mater.*, 2005, **17**, 1466–1471.
- 21 A. Herland, P. Björk, P. R. Hania, I. G. Scheblykin and O. Inganäs, *Small*, 2007, **3**, 318–326.
- 22 M. Hamed, A. Herland, R. H. Karlsson and O. Inganäs, *Nano Lett.*, 2008, **8**, 1736–1740.
- 23 M. Hedhammar, A. Rising, S. Grip, A. S. Martinez, K. Nordling, C. Casals, M. Stark and J. Johansson, *Biochemistry*, 2008, **47**, 3407–3417.
- 24 G. Askarieh, M. Hedhammar, K. Nordling, A. Saenz, C. Casals, A. Rising, J. Johansson and S. D. Knight, *Nature*, 2010, **465**, 236–238.
- 25 S. Grip, J. Johansson and M. Hedhammar, *Protein Sci.*, 2009, **18**, 1012–1022.
- 26 C. Fredriksson, M. Hedhammar, R. Feinstein, K. Nordling, G. Kratz, J. Johansson, F. Huss and A. Rising, *Materials*, 2009, **2**, 1908–1922.
- 27 M. Hedhammar, H. Bramfeldt, T. Baris, M. Widhe, G. Askarieh, K. Nordling, S. von Aulock and J. Johansson, *Biomacromolecules*, 2010, **11**, 953–959.
- 28 R. H. Karlsson, A. Herland, M. Hamed, J. A. Wigenius, A. Åslund, X. Liu, M. Fahlman, O. Inganäs and P. Konradsson, *Chem. Mater.*, 2009, **21**, 1815–1821.
- 29 R. M. Miriani, M. R. Abidian and D. R. Kipke, *Proc. IEEE Eng. Med. Biol. Soc.*, 2008, 1841–1844.
- 30 M. Åslund, E. Thaning, J. Lundberg, A. C. Sandberg-Nordqvist, B. Kostyszyn, O. Inganäs and H. von Holst, *Biomed. Mater.*, 2009, **4**, 045009.
- 31 K. P. R. Nilsson, P. Hammarström, F. Ahlgren, A. Herland, E. A. Schnell, M. Lindgren, G. T. Westermark and O. Inganäs, *ChemBioChem*, 2006, **7**, 1096–1104.
- 32 A. Herland, D. Thomsson, O. Mirzov, I. G. Scheblykin and O. Inganäs, *J. Mater. Chem.*, 2008, **18**, 126–132.
- 33 M. R. De Giorgi and A. Cerniani, *Dyes Pigm.*, 1991, **15**, 47–55.
- 34 G. Seu, *Dyes Pigm.*, 1993, **23**, 267–273.
- 35 A. O. Patil, Y. Ikenoue, N. Basescu, N. Colaneri, J. Chen, F. Wudl and A. J. Heeger, *Synth. Met.*, 1987, **20**, 151–159.
- 36 M. Widhe, H. Bysell, S. Nystedt, I. Schenning, M. Malmsten, J. Johansson, A. Rising and M. Hedhammar, *Biomaterials*, 2010, **31**, 9575–9585.
- 37 C. Riekel, C. Bränden, C. Craig, C. Ferrero, F. Heidelberg and M. Müller, *Int. J. Biol. Macromol.*, 1999, **24**, 179–186.
- 38 H. Somashekarappaa, V. Annaduraimb, Sangappa, G. Subramanyac and R. Somashekar, *Mater. Lett.*, 2002, **53**, 415–420.
- 39 C. Wang, K. Fang and W. Ji, *Fibres Polym.*, 2007, **8**, 225–229.
- 40 N. Y. Dang, W. Ma, S. F. Zhang, B. T. Tang and J. Z. Yang, *Text. Res. J.*, 2010, **80**, 374–382.

-
- 41 M. Li, Y. Guo, Y. Wei, A. G. MacDiarmid and P. I. Lelkes, *Biomaterials*, 2006, **27**, 2705–2715.
- 42 Y. Liu, X. Liu, J. Chen, K. J. Gilmore and G. G. Wallace, *Chem. Commun.*, 2008, 3729–3731.
- 43 M. H. Bolin, K. Svennersten, X. Wang, I. S. Chronakis, A. Richter-Dahlfors, E. W. H. Jager and M. Berggren, *Sens. Actuators, B*, 2009, **142**, 451–456.
- 44 K. D. McKeon, A. Lewis and J. W. Freeman, *J. Appl. Polym. Sci.*, 2010, **115**, 1566–1572.
- 45 E. W. H. Jager, E. Smela and O. Inganäs, *Science*, 2000, **290**, 1540–1545.
- 46 M. Asplund, PhD thesis, KTH, 2009.
- 47 L. Ding, M. Jonforsen, L. S. Roman, M. R. Andersson and O. Inganäs, *Synth. Met.*, 2000, **110**, 133–140.